A Black Hole in the Living Room

Werner Benger[1], Brad Corso[1], Erin Gillilan[1], and Manuel Tiglio[1]

Center for Computation & Technology at Louisiana State University, Baton Rouge, LA 70820, USA,
light@cct.lsu.edu,
http://www.cct.lsu.edu/

Abstract. We present a novel approach for studying a curved spacetime in a holistic, but still intuitive way. Using this approach, laymen and newcomers have a way to comprehend the properties of curved space without knowledge of the abstract mathematical formalism of non-euclidean spaces. Moreover, certain phenomena observable in astronomy can be demonstrated via familiar objects.

1 Introduction

The concept of curved spacetime is the core part of general relativity, but frequently people interested in relativity are deterred by its abstract mathematical formalism. Visual representations, if used at all, frequently lack appropriateness or are only accessible for scientists that work long in their specific field (see e.g. [1]). Depictions used in Hollywood movies are often based on simplified scientific visualizations that are used out-of-context. It is frequently heard that the general audience would not even appreciate physically correct visualizations. We do not adhere to this opinion and instead claim that a physically correct depiction of general relativistic phenomena transports much more realism, even on an unconscious level, resulting in an ultimately higher tension. Still, it is possible to communicate the properties of curved spacetime in an intuitive manner without the overhead of abstract mathematics by choosing proper visualizations. In particular as the theory of general relativity is a theory of geometry, it is representable by geometrical means. Applying these geometrical means to an familiar environment appears essential in this respect, and this is the path followed in this presentation.

We also note that some of the techniques discussed here might also be applied for situations beyond general relativity. It was shown that an optically active medium with spatial varying index of refraction can be described by the means of general relativity [2]. Recently it was speculated that even artificial black holes could be created via fluids [3], thus some of the experiments performed here in a virtual lab could possibly be examined in a real lab sometime in the future.

The tool used in our work is the `Light++` raytracer [4], which has its roots in the early 1990's. It is a self-standing rendering engine and as such free from any constraints imposed by standards such as OpenGL. Virtual reality languages, such as VRML or X3D, are used to display explicitly modeled objects or to visualize the result of a simulation performed elsewhere. In contrast, `Light++` allows to directly model a physical phenomena and yields a visual result based on the implemented laws of physics. Hereby the boundary among visualization and simulation vanishes, as the visualization is a simulation itself.

1.1 Previous Work

The most prominent application of Einstein's concept of curved space the gravitational field of a black hole. According to general relativity, a black hole has no more than three properties: mass M, electrical charge Q and angular momentum J. There are no other types of black holes with more properties. The most simple type with no electrical charge and no angular momentum is known as a static or Schwarzschild-type black holes.

Early investigations of the optical appearance of a black hole [5] were quite abstract. The evolution of computer graphics allows pedagogically superior presentations, like the surface of a neutron star [6]. Especially the astrophysical group in Tuebingen, Germany has a long history [7,8,9] in using ray-tracing to visualize curved spacetimes. Nowadays numerous implementations for the ray-tracing of Schwarzschild-type black holes exists, a good review can be found in [10]. Most approaches simulate a black hole in an astrophysical environment. In contrast, [11] simulated a black hole in an intuitively comprehensibly environment. Recently, [12] created a plugin using a fast hyperbolic approximation similar to [13] for use in the framework of the commercial software environment Maya.

Electrically charged black holes are unlikely to exist, but provide a simple testbed for rotating black holes. They where extensively discussed by [14] and recently [15] implemented the real-time raytracer BHFS ("Black Hole Flight Simulator") to allow interactive photo-realistic exploration of their complex topology embracing multiple parallel universes.

Rotating black holes are significantly more complex; their optical effects have been investigated by [16]. The raytracing technique is also used beyond computer graphics for scientific applications, for instance to compute the spectra of accretion disks [17] for astrophysical observations, and [18] coupled a ray-tracing code for a rotating black hole with a relativistic hydrodynamic code to find quasi-periodic oscillations in the spectrum. Only recently the visual distortions of a rotating black hole have been applied to a natural environment [19], which is didactically superior to reach a larger audience.

2 Physical Background

Curved spacetime is modeled via the mathematical formalism of Riemannian geometry [20,21]. It employs a metric tensor field to describe the geometrical properties of space and time. The theory of general relativity [22,23] provides a differential equation to compute the metric tensor for a spacetime in dependence of distribution of matter and energy. The first solution of the Einstein field equations of gravity has been found by Karl Schwarzschild. It describes a spherically symmetric vacuum spacetime. Using spherical coordinates t, r, ϑ, φ, the metric tensor has the form:

$$ds^2 = (1 - \frac{2m}{r})dt^2 - \frac{1}{1 - \frac{2m}{r}}dr^2 - r^2 d\vartheta^2 - r^2 \sin^2 \vartheta d\varphi^2 \quad . \tag{1}$$

The parameter m in Schwarzschild's metric corresponds to a mass[1] in this spacetime concentrated in a single point at $r = 0$. As we see immediately, something weird happens at the location where the radial distance r gets close to $2m$: the temporal metric component g_{tt} becomes zero here, while the radial component g_{rr} becomes infinite. Descriptively this means that

1. time comes to a standstill at $r = 2m$, i.e. objects appear frozen at this location,
2. radial distances become infinite at $r = 2m$, i.e. a rope hanging radially down would need to be infinitely long to reach downward to $r = 2m$.

However, nothing particular happens with the angular metric components $g_{\vartheta\vartheta}, g_{\varphi\varphi}$ at $r = 2m$, so the region $r = 2m$ is just a sphere with a finite circumference of $2\pi r$ and a surface area of $4\pi r^2$. Thus, a disk built around the black hole (imagine a donut-like space station) with a certain radial coordinate extension dr will have an extremely large radial physical extension $ds = \sqrt{1/(1 - \frac{2m}{r})}\, dr$, approaching infinity towards $r = 2m$, whereas its circumference changes as usually known in flat space just linearly with r. By this depiction we see that the physically measurable relationship between radius and circumference is no longer 2π as in Euclidean space, but something else (approaching infinity), reflecting a crucial difference of curved space. At this point we will not discuss what happens when $r < 2m$ when the radial metric component becomes negative, that will be addressed elsewhere.

2.1 Photo-realistic Visualization

To achieve a fully covariant visualization of a curved space, we need to consider what an observer actually could measure, in contrast to the appearance of various quantities in a random coordinate system. It is self-evident to pose the question what an observer actually would *see* in a curved spacetime. Tackling this task requires to trace the path of light rays in a curved spacetime and to model its interaction with test objects. Such test objects are essential since a pure vacuum would otherwise not contain any visible light at all; on the other hand, we need to model these test objects in an unphysical manner as massless such that we can keep the simple Schwarzschild solution.

[1] using geometrical units, i.e. $m = GM/c^2$ with c the speed of light, G the gravitational constant and M the mass in usual units. Any mass can be expressed as a geometrical distance by virtue of G and c.

The path of light in a curved spacetime is a lightlike curve connecting two points in by minimal or maximal length. Such a curve $q(s)$ is called a lightlike geodesic and is determined by the geodesic equation

$$\frac{d^2 q^\lambda}{ds^2} + \Gamma^\lambda_{\mu\nu} \frac{dq^\mu}{ds} \frac{dq^\nu}{ds} = 0 \tag{2}$$

where $\Gamma^\lambda_{\mu\nu}$, the so-called Christoffel symbols, are an abbreviation for an expression formed from the metric tensor and its first partial derivatives:

$$\Gamma^\lambda_{\mu\nu} := \frac{1}{2} g^{\lambda\alpha} \left(\frac{d\, g_{\mu\alpha}}{dx^\nu} + \frac{d\, g_{\nu\alpha}}{dx^\mu} - \frac{d\, g_{\mu\nu}}{dx^\alpha} \right) \quad . \tag{3}$$

Investigation of the solutions of the geodesic equation eq. (2) shows that light is attracted by black holes similar to planets and comets traversing in the solar system. This deflection of light is two times as large as predicted by Newtonian theory. Its observational verification during a sun eclipse lead to the break through of general relativity.

3 Results

We model a virtual scene similar to that one in [11]. The objects contained within the scene mainly serve as recognizable orientation points. To introduce a notion of time, a light source with periodic modulation is added. The light source blinks in an intense red flash which illuminates the environment as well.

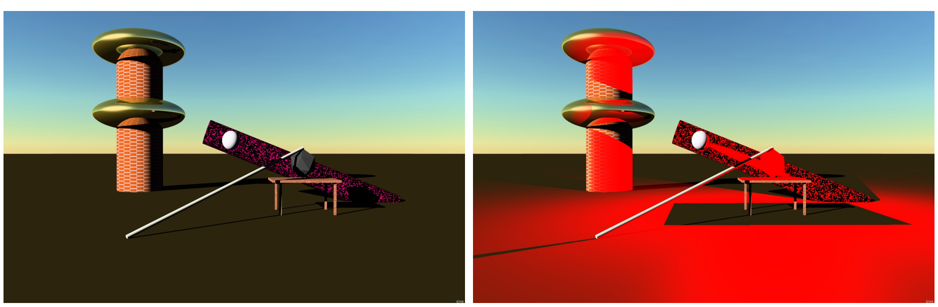

Fig. 1. The virtual scene used for inspecting the curved spacetime. The icosaedron placed on the desk periodically blinks in intense red light.

3.1 Light Wavefronts

Even in the context of special relativity, the effect of the finite speed of light on the appearance of fast moving objects had not been considered until 1959 and led to the discussion whether the Lorentz contraction, though definitely measurable, is observable at all [24].

To explore such visual consequences, we model the finite speed of light also in our rendering software. This violates many assumptions which are built into common rendering algorithms. Only few such implementations exist, but some experiments [25] even modeled the decreased speed of light in refractive media. Here, we concentrate on the effects of indirect illumination, to extend what has been modeled also by [26]. When light has an infinite speed we see things in

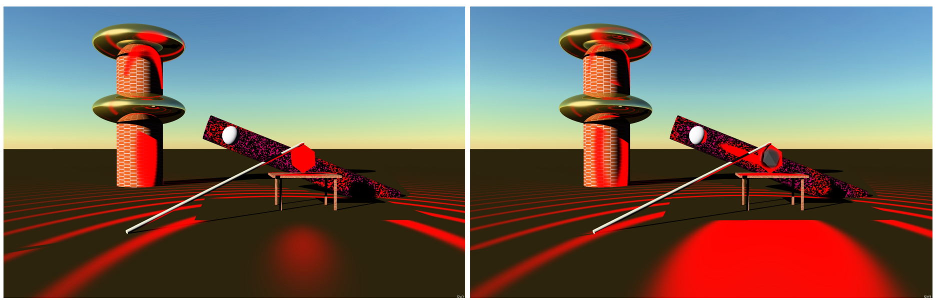

Fig. 2. Simulating a low, finite speed of light, we see the blinking light source casting many visible wavefronts.

the present tense - meaning that we see what is happening at the time that it happens no matter how far away the event occurred. But considering a finite speed of light we are always looking back into the past – all light must travel a distance to get to our eye, requiring time. This results in prominently visible consequences: if there are multiple paths that the light can travel to get to our eye, we see each such path referring to a different instance in time at their origin. In Fig. 2 obviously the shortest path from the light emitting object to the observer is a straight line. Thus we first see the object lighting up in red, while the floor still remains in darkness. Shortly later, when the emitter itself has already faded, a front of illumination still wanders along the floor. This "wave front" is caused by the diffuse reflection of light, which we see with increasing time delay. This is in contrast to the case of infinite speed of light, where a flash illuminates the entire scene at once.

The more we decrease the speed of light, the more numerous and the sharper the wave fronts become. In this scenario, light indeed appears like a wave, like ripples in water after a stone has been thrown in. There the waves of a water surface propagate concentric around the point of origin, i.e. independent of the observer. However, light waves are concentric around the point of specular reflection - and thus dependent on the observer's location.

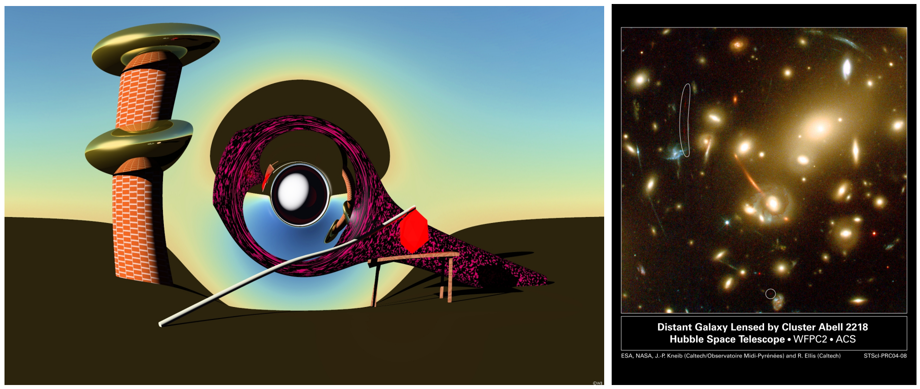

Fig. 3. Introducing general relativistic curvature of space into the scene, as if the white ball in the center corresponds to the surface of a black hole. Gravitational redshift has been intentionally ignored in this rendering.

3.2 Gravitational Lensing

"Gravitational lensing" is caused by the gravitative attraction of light and actually observable in nature. It is helpful to retrieve information about astrophysical objects and the universe itself. In the scene depicted in Fig. 3 we observe a black hole with a diameter of 0.5m from a distance of 25m; such a black hole corresponds to the mass of the planet Saturn. When multiple astrophysical objects are observed with identical surface intensity and color, this is strong evidence for gravitational lensing of a single source. We see the same effect in our virtual scene with the red light source, which appears twice. Both images experience different magnifications, similar to a remote galaxy as lensed and eventually becoming visible due to lensing by a massive foreground object (e.g. [27]).

A consequence of the light attraction is that the entire surface of the black hole is visible from any point of view. It is impossible to "hide" behind a black hole [28]. Strictly speaking, this would also affect the illumination of the scene, but we intentionally ignore this effect here.

3.3 Bending of Light

Curved spacetime not only allows us to see a certain object multiple times, but also to see it from different perspectives. In the case of the desk that our ikosaedron is resting on, the primary image (Fig. 4, right) displays the side view, while the secondary image shows the upper surface (Fig. 4, left). Note that a fully three-dimensional scene needs to be modeled for this effect to become visible - the different perspectives could not be achieved by applying a 2D filter like a "photoshop plugin". to a background photograph. Note that the images in Fig. 4 are not to scale. Actually, the secondary image is much smaller than the primary one (see Fig. 3 for a direct comparison). Using our intuition from flat space, this

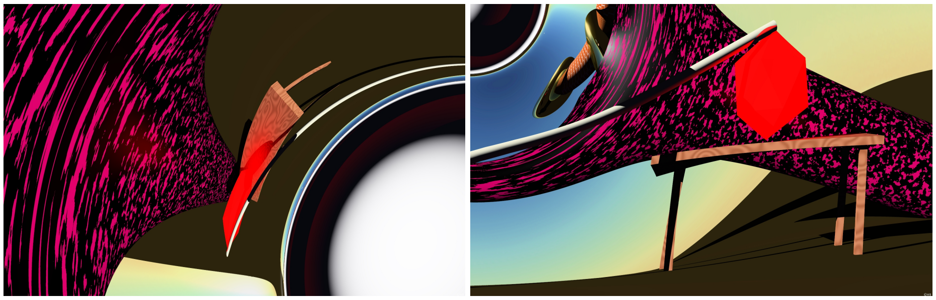

Fig. 4. The primary and secondary image of the light source on the desk; we see the desk from another perspective.

can be interpreted as the secondary image being further away than the primary one. This intuition is well supported by the finding of the parallax angle is smaller for the secondary image, as presented in [29]. The ability to employ a stereographic display fully supports this finding even for viewers without a-priori knowledge of relativity and curved spacetime.

3.4 Time Delay of Secondary Images

Due to the longer path that the light rays responsible for the secondary image traveled on, we are effectively looking further back in time than when viewing the primary image. especially as light travels slower in the vicinity of the black

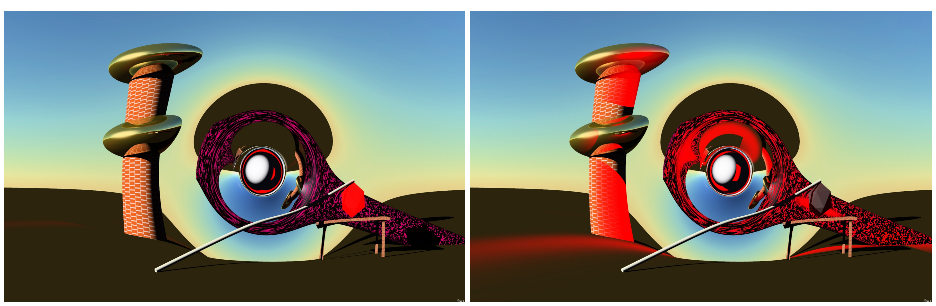

Fig. 5. Taking into account the finite speed of light, the blinking flash of the light source becomes first visible on the primary image. The secondary image does not flash until the primary image becomes dark again.

hole. This is known as the Shapiro effect [30]. It has been observed in nature in great precision. In our virtual scene, this effect occurs in a delayed blinking of the secondary image, as depicted by Fig. 5. The flash of the secondary image becomes visible at the same time as the brick cylinder in the back ground becomes enlightened. This indicates that the visual (proper) distance of the secondary image is equal to the proper distance of the brick cylinder, i.e. it looks further away than the primary image. This impression is successfully communicated by stereographic viewing of the same scene [29].

3.5 Gravitational Redshift

The metric component g_{tt} causes time to run slower in the vicinity of a large mass, causing redshift of light leaving a gravitational field. The effect was measured on earth using high-precision atomic clocks and must be taken into account for the global positioning system to work in the desired precision.

While we could employ some color shift model such as the "dominant wavelength model" used by [31] for visualization, we found an alternative. We note that every motion slows down, including the apparent motion of light wave fronts. It takes infinite time for a photon to reach an outside observer from the event horizon, thus any light observed originating there stems from the far past. Wave fronts of light pulses will thus "pile up" at the horizon: a (static) membrane enveloping the black hole just outside the horizon will reflect pulses in the past as well as recent ones, as depicted in Fig. 6.

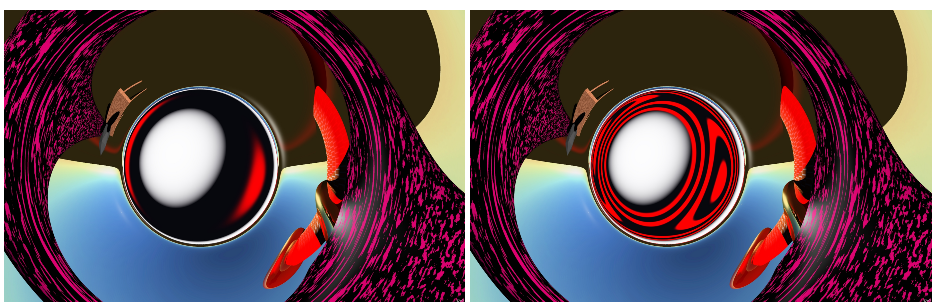

Fig. 6. Membrane radii of $r = 0.55, 0.505$ for an event horizon at $r = 0.5$. The time dilation allows us to see echoes of light pulses from far in the past.

At some times we see the surface illuminated, at others it appears dark, leading to a zebra-like pattern that moves over the surfaces. New light pulses appear on one pole of the surface and disappear on the anti-pole. This would also be the case if the membrane was homogeneously emitting pulsating light itself; with incident light this effect doubles. We see rings of wavefronts traveling over the membrane, each front corresponding to a pulse of the light source in the past. The rings become more numerous and sharper the closer the membrane is to the actual event horizon at $r = 2m$. If it were at the horizon itself, we would see an infinitely dense echo of all light pulses that have ever been emitted by the light source. An alternative, but equivalent interpretation of the visual effect is that the membrane is infinitely far away from the observer.

4 Conclusion

We have demonstrated how a physically modeled virtual reality can be used to provide a deeper comprehension of curved space. Various components of a metric tensor field constituting curved space lead to certain visual effects that represent these. Fig. 3 and Fig. 4 depict a static scene and can be seen of a visualization of curved space, or the metric components $g_{rr}, d\Omega$ only. Fig. 5 and Fig. 6 introduce a dynamic component and thereby provide a visualization of g_{tt}. In the case of the Schwarzschild metric, $g_{tt} = -1/g_{rr}$, so the information content is identical. However, in the case of more complex gravitational fields, especially those of rotating black holes, we may expect another visual quality.

5 Acknowledgements

First of all we especially thank Yaakoub El Khamra for his immense support on managing the rendering jobs on various supercomputing resources, and Marcel Ritter for providing sophisticated camera paths. This research employed the resources of the Center for Computation and Technology at Louisiana State University, which is supported by funding from the Louisiana legislature's Information Technology Initiative. We thank Brian D. Ropers-Huilman for providing fast and unbureaucratic support. Valuable suggestions are due to deep discussions with Andrew Hamilton, University of Colorado, Boulder. This work was partially supported by the NSF under grant PHY0505761 and by the National Center for Supercomputer Applications under grant MCA02N014.

References

1. Benger, W.: Visualization of General Relativistic Tensor Fields via a Fiber Bundle Data Model. PhD thesis, Free University Berlin (2004)
2. Gordon, W.: Zur Lichtfortpflanzung nach der Relativitätstheorie. Annalen der Physik **72** (1923) 421–456
3. Novello, M., Visser, M., Volovik, G., eds.: Artificial Black Holes. World Scientific Publishing (2002)
4. Benger, W.: The light++ raytracing library. `http://www.photon.at/~werner/light/` (1990-2005)
5. Cunningham, C.T.: Optical appearance of distant objects to observers near and inside a Schwarzschild black hole. Physical Review D **12** (1975) 323–328
6. Nemiroff, R.J.: Visual Distortions Near a Black Hole and Neutron Star. American Journal of Physics **61** (1993) 619+
7. Zahn, C.: Vierdimensionales Ray-Tracing in einer gekrümmten Raumzeit. Master's thesis, Institut für Theoretische und Angewandte Physik Universität Stuttgart (1991)
8. Weiskopf, D.: Visualization of Four-Dimensional Spacetimes. PhD thesis, Universität Tübingen (2001)
9. Weiskopf, D.: Four-Dimensional Non-Linear Ray Tracing as a Visualization Tool for Gravitational Physics. In Ertl, T., Hamann, B., Varshney, A., eds.: Visualization '00, ACM Press (2000) 445–448

10. Perlick, V.: Gravitational Lensing from a Spacetime Perspective. Living Rev. Relativity (7) (2004) `http://www.livingreviews.org/lrr-2004-9/`, cited on 1. Dec. 2005.
11. Benger, W.: Simulation of a black hole by raytracing. In F.W. Hehl, R.P., Ruder, H., eds.: Relativity and Scientific Computing - Computer Algebra, Numerics, Visualization, Berlin Heidelberg New York, Springer Verlag (1996) 2–3
12. Ritter, M.: Rendering Black Holes in Maya. 2nd High-End Visualization Workshop, Obergurgl (2005) `http://astro.uibk.ac.at/visworkshop2005/talks/MayaBlackHole.pdf`.
13. Benger, W.: Raytracing using hyperbolic light paths. Presented during the Alpbach Summer School of the Austrian Space Agency (1992)
14. Metzenthen, W.E.: Appearance of distant objects to an observer in a charged-black-hole spacetime. Physical Review D **42** (1990) 1105–1117
15. Hamilton, A.: Black hole flight simulator. AAS 204th Meeting (2004) Session 78 Informal Astronomy Programs.
16. Pineault, S., Roeder, R.C.: Applications of Geometrical Optics to the Kerr Metric. Analytical Results. Astrophysical Journal **212** (1977) 541–549
17. Müller, A., Camenzind, M.: Relativistic emission lines from accreting black holes. The effect of disk truncation on line profiles. Astronomy and Astrophysics **413** (2004) 861–878
18. Schnittman, J., Rezzolla, L.: Quasi-periodic Oscillations in the X-ray Light Curves from Relativistic Tori. ApJ, Letters, in press (2005) `astro-ph/0506702`.
19. Gipson, B., Kornreich, D.A.: Visualizing Black Holes. American Astronomical Society Meeting Abstracts **206** (2005)
20. Eisenhart, L.: Riemannian Geometry. Princeton University Press (1949)
21. O'Neill, B.: Semi-Riemannian Geometry, with applications to Relativity. Academic Press, Inc. (1983)
22. Einstein, A.: Die Grundlage der allgemeinen Relativitätstheorie. Annalen der Physik **4**(49) (1916) 284–339 available on the Albert Einstein Archives of the Jewish National and University Library/ the Hebrew University of Jerusalem, Archival call No. 120-788, `http://www.alberteinstein.info/gallery/pdf/CP6Doc30_pp284-339.pdf`.
23. N.Straumann: General Relativity and Relativistic Astrophysics. Second edn. Springer Verlag Berlin (1991)
24. Terrell, J.: Invisibility of the lorentz contraction. Physical Review **116**(4) (1959) 1041–1045
25. Li, J., Shum, H.Y., Peng, Q.: An improved spacetime ray tracing system for the visualization of relativistic effects. In: Eurographics 2001. (2001)
26. Savage, C., Searle, A.: Visualising special relativity. The Physicist **36** (1999) 141
27. Kneib, J.P., Ellis, R.S., Santos, M.R., Richard, J.: A Probable z $\sim$7 Galaxy Strongly Lensed by the Rich Cluster A2218: Exploring the Dark Ages. Astrophysical Journal **607** (2004) 697–703
28. Jackson, M.: Two black hole holography, lensing, and intensity. Physical Review D **64** (2001)
29. Benger, W., Seidel, E.: Stereographic rendering of curved space. Presented at Supercomputing 2005, Seattle (2005)
30. Shapiro, I.I.: Fourth test of general relativity. Phys. Rev. Lett. (13) (1964) pp.789–791
31. Weiskopf, D., Kobras, D., Ruder, H.: Real-World Relativity: Image-Based Special Relativistic Visualization. In T.Ertl, B., A.Varshney, eds.: Visualization '00, ACM Press (2000) 303–310